Head movements quadruple the range of speeds encoded by the insect motion vision system in hawkmoths

Shane P. Windsor* Graham K. Taylor†

*Department of Aerospace Engineering, University of Bristol, University Walk, Bristol, BS8 1TR, UK
†Department of Zoology, University of Oxford, Oxford OX1 3PS, UK

Author for correspondence: Graham K. Taylor; email: graham.taylor@zoo.ox.ac.uk

Proc. R. Soc. B 20171622. http://dx.doi.org/10.1098/rspb.2017.1622

Abstract

Flying insects use compensatory head movements to stabilize gaze. Like other optokinetic responses, these movements can reduce image displacement, motion, and misalignment, and simplify the optic flow field. Because gaze is imperfectly stabilized in insects, we hypothesised that compensatory head movements serve to extend the range of velocities of self-motion that the visual system encodes. We tested this by measuring head movements in hawkmoths *Hyles lineata* responding to full-field visual stimuli of differing oscillation amplitudes, oscillation frequencies, and spatial frequencies. We used frequency-domain system identification techniques to characterise the head's roll response, and simulated how this would have affected the output of the motion vision system, modelled as a computational array of Reichardt detectors. The moths' head movements were modulated to allow encoding of both fast and slow self-motion, effectively quadrupling the working range of the visual system for flight control. By using its own output to drive compensatory head movements, the motion vision system thereby works as an adaptive sensor, which will be especially beneficial in nocturnal species with inherently slow vision. Studies of the ecology of motion vision must therefore consider the tuning of motion-sensitive interneurons in the context of the closed-loop systems in which they function.

Keywords: head movements; eye movements; gaze stabilization; motion vision; elementary motion detector; flight control

1 Background

Eye movements are essential to shifting, fixating, and stabilizing gaze [1–3]. Gaze stabilization is especially challenging in agile flight, and as their eyes are fixed to the head, flying insects use head movements to stabilize the retinal image. Hengstenberg *et al.* [4] identified three distinct functions of these compensatory head movements, which were to reduce the displacement, motion, and misalignment of the retinal image. In addition, by simplifying the optic flow generated by the insect's own self-motion, compensatory head movements can also simplify the visual processing needed to estimate structure from motion [1]. Gaze stabilization is most effective about the longitudinal roll axis, but is rarely complete, typically operating at gains less than one. This is usually assumed to reflect the constraints associated with ensuring

stable feedback in the presence of delay, because negative feedback systems become unstable at gains above one if the phase shift reaches 180° [4]. Yet whilst it is clearly important to maintain a suitable gain margin in the presence of substantial phase shift, compensatory head movements exhibit little or no phase delay in free flight [5,6]. Thus, an alternative explanation of the low gain of compensatory head movements is that their primary function is to match the retinal image speed to the performance of the motion vision system [4]. Mentioned briefly in a recent review of gaze stabilization [3], this explanation has received almost no attention since it was proposed [4], and has not been explored quantitatively to our knowledge.

Motion vision is central to insect flight control, because the optic flow field provides detailed information on the insect's self-motion and the structure of its environment [7]. This information is encoded locally by arrays of elementary motion detectors (EMDs), whose output is combined to sense the global optic flow. Multiple lines of evidence from neuroanatomy [8,9], neurophysiology [10,11], and behaviour [12,13] indicate that the EMDs implement a kind of correlation-type detector called a Reichardt detector [14]. These sense motion but do not respond linearly to stimulus speed [11–15]: when presented with a steadily moving stimulus, the steady-state output of a Reichardt array increases with increasing stimulus speed until reaching a peak and decreasing. The actual output depends on the spatial frequency and contrast of the stimulus, and for a given spatial frequency is most closely related to the contrast frequency, defined as the number of luminance cycles passing a point in the visual field per unit time [13,15]. The effect of these nonlinearities is even more pronounced in response to dynamic stimuli. For example, when presented with a sinusoidally-oscillating grating, the time-varying output of a Reichardt array will only approximate a sinusoid if the contrast frequency stays within the range over which EMD output is a monotonically increasing function of contrast frequency: outside this range, the output becomes distorted [16]. Something similar occurs in response to a stimulus with a white-noise velocity profile [11], and in both cases the gain decreases as the standard deviation of the contrast frequency increases [11,16].

It is not surprising, therefore, that EMD responses are matched closely to visual ecology [17–19]. For instance, motion-sensitive visual interneurons taking input from the EMDs have a slower response in nocturnal than diurnal species, and have a slower response in species which hover [17–21]. What is surprising is how little attention has been paid to the effect of head movements in modulating these responses when the motion vision system is operating in closed-loop [22]. This is important, because whereas it is usually assumed that the dynamic range of the motion vision system is tuned by adjusting the intrinsic spatiotemporal properties of the EMDs [16,18], compensatory head movements could offer a dynamic mechanism for achieving the same end [3]. Here we characterise the compensatory head movements made by hawkmoths in response to full-surround visual roll stimuli presented whilst the moths were flying tethered in a sustained physiological flight state. We then embed the dynamics of the experimentally-measured head motions within a computer simulation of the hawkmoth visual system, and use this to examine how compensatory head movements affect the effective working range of the moths' motion vision. We conclude by exploring the wider implications of our findings for the ecology of motion vision.

2 Methods

We used a virtual-reality flight simulator to present white-lined hawkmoths *Hyles lineata* with full-surround visual stimuli, during a series of tethered flight experiments in which we varied the frequency (f), amplitude (A), or spatial frequency (S) of a sinusoidally oscillating grating stimulus about the moths' roll axis (Fig. 1). The experiments that we describe overlap with a series of tests reported previously in relation to the measured force-moment responses [23], but the accompanying head movements were measured for a subset of individuals, and are reported here for the first time.

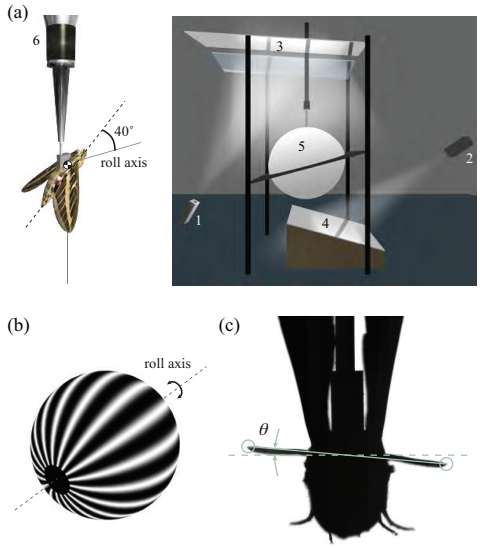

Figure 1. Experimental setup. (a) Full-surround visual stimuli were provided by two modified data projectors (1,2) back-projecting images via mirrors (3,4) onto a hollow acrylic sphere (5). The moth was tethered at the centre of the sphere to a six-component force transducer (6), with its body tilted at 40° to the horizontal. (b) Visual stimulus, comprising a spherical sinusoidal grating rotating sinusoidally about the horizontal roll axis. (c) Estimation of head roll angle (θ) from line joining antenna tips (circled).

2.1 Behavioural experiments

The $n = 7$ moths were rigidly tethered at the centre of a 1m diameter hollow acrylic sphere (Fig. 1a) onto which we back-projected moving full-field stimuli (Fig. 1b). Each stimulus comprised a spherical sinusoidal grating, oscillating sinusoidally about the moth's horizontal roll axis, with a dark circle subtending 20° at the poles to avoid aliasing (Fig. 1b). We varied the mean contrast frequency (c) of the stimulus by adjusting its oscillation frequency, $f \in \{1, 2, 3, 4, 6, 8, 12 \text{ Hz}\}$, amplitude $A \in \{2.5°, 5°, 10°, 20°, 30°\}$, or spatial frequency $S \in \{(40°)^{-1}, (20°)^{-1}, (10°)^{-1}, (6°)^{-1}, (3°)^{-1}\}$. We varied one parameter at a time, from reference values of $f = 2$Hz, $A = 5°$, and $S = (20°)^{-1}$ designed to give a $c = 2$Hz mean contrast frequency coinciding with the peak steady-state response of the moths' EMDs (Fig. 2). The contrast frequency describes the number of luminance cycles passing a given point in the visual field per unit time: this quantity varies with time for a sinusoidally oscillating grating, but over a complete oscillation cycle the mean contrast frequency is proportional to the frequency and amplitude of the oscillation, with $c = 4fAS$. Each stimulus set was presented as a block, and we randomized the order of these blocks and the test conditions within them. The stimuli that we used represent slices through the possible set of combinations of oscillation frequency, oscillation amplitude, and spatial frequency, centred on the estimated peak response of the moths' EMDs. Whilst this does not guarantee that any of the stimuli that we presented actually coincided with the true peak response of the moths' EMDs (which would have required us to present many more combinations than was possible within the moths' viable flight time), centring the slices on the estimated peak ensures that we tested each of the parameters within a biologically relevant range.

The moths were first flown 2 to 3 days post-eclosion, on up to 3 days in total, and were given 0.5 h to acclimate to the dim lab light levels and 26°C lab temperature. Each moth was removed from the simulator at the end of the experiment, fed honey solution until sated, then stored overnight on its tether at 12°C. We presented each stimulus for at least 60s with the moth in sustained continuous flight,

during which time we recorded 28s of high-speed video. The moths were shown a white background in the 30s between stimulus presentations. We filmed the moths in silhouette at 500fps under 850nm infrared illumination (Fig. 1c), with the camera looking in through a small porthole behind the insect. We estimated the roll angle of the head from the line joining the tips of the antennae (Fig. 1c), which we tracked by moving a user-defined tip template within a local search area centred on the position of the tip in the preceding frame. The wings obscured the antennae for a small proportion of each stroke, but as the wingbeat frequency was a factor of three greater than the highest stimulus frequency, the few missing data points were easily estimated by interpolation. We undertook validation tests to confirm that the antennal motor system did not respond to the stimulus by moving the antennae independently of the head (see electronic supplementary material), and excluded any trials in which the head was yawed, as these would have degraded the accuracy of the head angle measurements. We transformed the head angle measurements into the frequency domain, and computed the magnitude, phase, and coherence of the response relative to the angular position of the stimulus, using the chirp Z-transform and Welch's windowing method [23]. We excluded responses with coherence <0.6 from the analysis, which is a recommended quality-control threshold for system identification [24]. In those cases where the same individual experienced the same stimulus more than once, we averaged the moth's responses to that stimulus before combining them with the responses from other individuals. Because some individuals could not be presented with, or did not respond to, all of the stimuli, we also calculated the marginal means for each test condition in a mixed model controlling for individual. In principle, these marginal means remove the effects of systematic inter-individual variation, but as they risk overfitting and were close to the simple means anyway, we present only the latter.

2.2 Computational model of motion vision

We built a computational model of the moth's motion vision system as a circular array of Reichardt detectors (Fig. 2a,b). We also tried modelling a spherical array, which gave similar results because the output was dominated by the high proportion of EMDs sampling the field of view equatorially. We varied the angular position of the grating relative to the head to simulate the sensory input experienced at the retina for any given combination of stimulus motion and head motion. Each EMD comprised two mirror-symmetric half-detectors sampling the outputs of a pair of adjacent ommatidia (Fig. 2a). We computed the light input to each ommatidium by passing the raw input image through a gaussian filter approximating an Airy disc with a half-width equal to the acceptance angle, simulating the optics of the moth's optical superposition eye. We modelled the photoreceptors' response to this input by forward-backward filtering it with a one-pole spatial high-pass filter, representing the adaptation of the visual system to ambient light levels by removing any slow-varying offset. The signal was then passed through a one-pole temporal low-pass filter, modelling the phase shift due to the finite response time of the photoreceptors. The output of each half-detector was computed by multiplying the outputs of the two ommatidia, having delayed one of these outputs using another one-pole temporal low-pass filter to achieve a unidirectional motion response (Fig. 2a). We calculated the EMD output by differencing the outputs of the two half-detectors to achieve a bidirectional motion response (Fig. 2a), then summed over all of the EMDs to determine the output of the array. We identified the amplitude and phase of the response to oscillatory stimuli by fitting a sinusoid at the stimulus frequency to the time-varying output of the array using simple harmonic regression: the corresponding R^2 value measures the goodness of fit of this sinusoid, and declines as the output becomes distorted by the various nonlinearities present in the system.

The parameters of the model were matched to the details of the moths' visual system (Table 1). The properties of a Reichardt array depend upon the delay time constant (τ), and the angular separation of the photoreceptor inputs, which for nearest-neighbour interactions is set by the interommatidial angle ($\Delta\psi$). To a first approximation, the steady-state response is expected to be maximal at a contrast frequency $c = (2\pi\tau)^{-1}$ for any given spatial frequency, and at a spatial frequency $S = (4\Delta\psi)^{-1}$ for

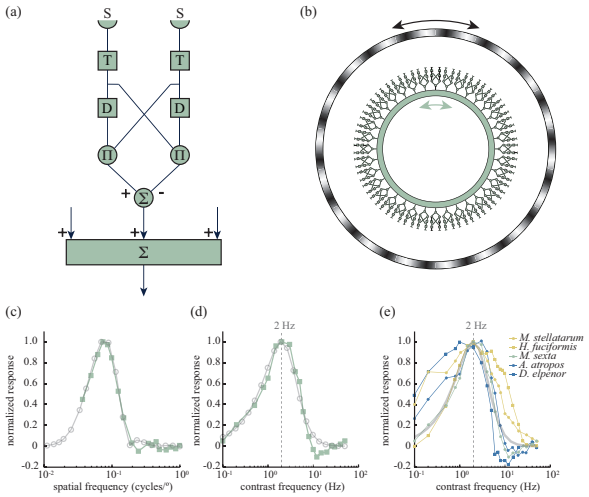

Figure 2. Computational model of motion vision. (a) Diagram of a single Reichardt detector, comprising two mirror-symmetric half-detectors. Light reaching the photoreceptors is passed through a spatial high-pass filter (S) and a temporal low-pass filter (T), before being split into the delay arm of one half-detector and the non-delay arm of the other. The delay is implemented by a temporal low-pass filter (D), and the delayed signal is multiplied by the non-delayed signal in the other arm (Π). After differencing the outputs from the half-detectors (Σ), the result is summed with the output of the other detectors in the array (Σ). (b) Diagram of complete array. Black arrows indicate stimulus motion; turquoise arrows represent head motion. (c,d) Comparison of array output (grey circles) with electrophysiological data (turquoise squares) to which the model was tuned [19]. (e) Electrophysiological data from the lobula cells of the diurnal (golden), crepuscular (turquoise), and nocturnal (blue) hawkmoths *Macroglossum stellatarum* [18], *Hemaris fuciformis* [17], *Manduca sexta*, *Acherontia atropos*, and *Deilephila elpenor* [19]. The thick grey line shows the tuned response of our model, peaking at a contrast frequency of 2Hz.

Table 1. Parameters of model Reichardt array

variable	value
interommatidial angle ($\Delta\psi$)	1.0°
acceptance angle†	2.0°
spatial high-pass filter constant†	0.0075
temporal low-pass filter time constant†	46 ms
delay time constant (τ)†	46 ms

†free parameter fitted to electrophysiological data [19].

any given contrast frequency [13,15]. However, the response is also shaped by the filtering properties of the optics and the photoreceptors. In the absence of electrophysiological data from *H. lineata*, we tuned our model to published data [19] from optic-flow sensitive interneurons of the tobacco hawkmoth *Manduca sexta*. Electrophysiological data are available for a few more-closely related species [17–19], but as these are fully diurnal or nocturnal (Fig. 2e), it seems reasonable to take the crepuscular *M. sexta* as a model for the crepuscular *H. lineata*. Having fixed the interommatidial angle, we manually tuned the free parameters of our model (Table 1) until its steady-state response to a steadily rotating stimulus matched the electrophysiological data collected under similar test conditions (Fig. 2c,d).

The delay time constant and the time constant of the temporal low-pass filter summed linearly, acting as a single parameter to tune the contrast frequency, whilst the acceptance angle and spatial high-pass filter interacted to tune the spatial frequency response. In tuning the model, we matched the response leading up to the maxima in respect of spatial frequency and contrast frequency, rather than matching all aspects of the response at higher spatiotemporal frequencies. We did so because this section of the curve effectively delimits the useful working range of the array. The values of the fitted parameters were in the range expected from previous work, with the ratio of acceptance angle to interommatidial angle being close to 2, as is also the case in many crepuscular and nocturnal insects [25], and with the temporal parameters being similar to those estimated for other moth species which fly in low light conditions [20,21,26]. We undertook extensive validation tests to confirm the sensitivity of the model output to the parameters used (see electronic supplementary material), and found that the general trends present in the output were insensitive to the exact values of the parameters.

3 Results

The moths flew strongly in the flight simulator, producing time-averaged aerodynamic forces with a median magnitude 96% of body weight. The moths modulated the forces and moments in time with the stimulus, producing large roll moments in response to roll stimuli, together with a small but coherent yaw moment [23]. The moths also rolled their heads in time with the stimulus, and did so coherently under almost all of the test conditions (Fig. 3c,f,i), indicating that most of the spectral power in the head's motion at the stimulus frequency was linearly attributable to the stimulus.

3.1 Gaze stabilization depends upon contrast frequency

The gain of the moths' head motions, defined as the ratio of the roll angle amplitude of the head relative to the roll oscillation amplitude of the stimulus, increased with stimulus frequency, rising to a maximum of 0.96 at $f = 6$Hz, but dropped off quickly at higher frequencies (Fig. 3a). The bandpass properties of this response are similar to those of the optic-flow sensitive interneurons that drive it [17,19], and are typical of the optomotor responses of insects in general. The head moved in phase with the stimulus at the lowest oscillation frequencies, but the phase rolled off quickly as the stimulus frequency increased,

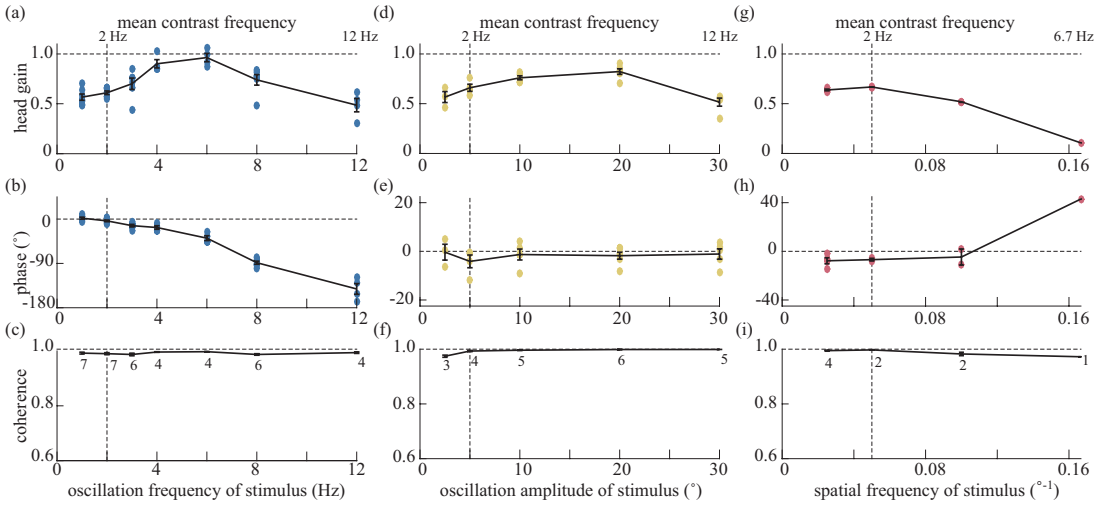

Figure 3. Measured head movements in tests varying the mean contrast frequency of the stimulus by varying the frequency (a-c), amplitude (d-f), or spatial frequency (g-i) of the stimulus. The gain and phase relate the angular position of the head to the angular position of the stimulus; the coherence measures the proportion of the spectral power that is linearly attributable to the stimulus at that frequency. Vertical dashed lines denote the reference test conditions; horizontal dashed lines denote the conditions for perfect gaze stabilization. Numbers beneath the points indicate the number of moths that responded with coherence greater than 0.6. Filled circles plot individual responses; error bars plot means ± one standard error, connected by straight line segments to aid visualisation.

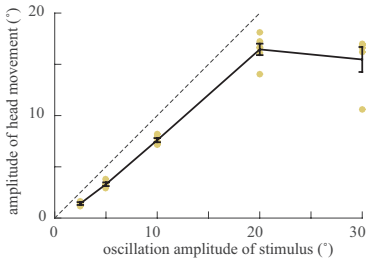

Figure 4. Amplitude of head movement measured in tests varying the stimulus amplitude. Filled circles plot individual responses; error bars plot means ± one standard error, connected by straight line segments to aid visualisation. Dashed line denotes unity gain.

becoming almost anti-phase by $f = 12$Hz (Fig. 3b). This roll-off is typical for a system with temporal filtering behaviour, but its near linearity with respect to frequency (Fig. 3b) is also consistent with the effects of a pure time delay of approximately 38ms (*cf.* Table 1).

The head's gain also increased with the oscillation amplitude of the stimulus, reaching a maximum at $A = 20°$, but dropping sharply beyond this (Fig. 3d). Linear systems have the property of homogeneity, meaning that doubling the input amplitude should double the output amplitude at a given frequency, so the amplitude dependence of the response magnitude is a clear indication of nonlinearity. This may be due partly to output saturation, because the amplitude of the measured head motion was statistically indistinguishable at stimulus amplitudes of $A = 20°$ and $30°$ (note overlapping error bars in Fig. 4). Output saturation cannot explain the nonlinearity at lower stimulus amplitudes, however, as both the

amplitude (Fig. 4) and gain (Fig. 3d) of the head movement increased consistently with oscillation amplitude for stimulus amplitudes $A < 20°$. Instead, it seems likely that the increasing gain at lower stimulus amplitudes was a direct effect of stimulus speed or contrast frequency, rather than oscillation amplitude *per se*. The phase of the response, in contrast, was rather insensitive to stimulus amplitude (Fig. 3e).

The gain and phase of the head motions did not vary much with the spatial frequency of the stimulus at spatial frequencies $S \leq (10°)^{-1}$ (Fig. 3g,h). However, only one moth responded coherently to a spatial frequency as high as $S = (6°)^{-1}$ (Fig. 3i), and even this moth showed a greatly diminished gain compared to its response at lower spatial frequencies (Fig. 3g,h). No moth responded with coherence greater than 0.6 to visual stimuli at the highest spatial frequency of $S = (3°)^{-1}$, either in terms of the measured head motion or the measured roll moment. This makes sense, because the compound eyes should not be able to resolve a grating with a wavelength less than 2°, given their 2° acceptance angle and 1° interommatidial angle [1]. The 3° wavelength of the $S = (3°)^{-1}$ stimulus would therefore be expected to fall close to the limits of their resolution.

3.2 Head movements only partially stabilize gaze

The extent to which compensatory head movements stabilize gaze depends upon both the gain (G) and phase (ϕ) of the response, which combine to form the complex gain $Z = Ge^{\phi i}$. Perfect tracking is achieved at unity gain and zero phase, corresponding to a complex gain $Z_0 = 1 + 0i$ (Fig. 5a). The degree to which gaze is stabilized is determined by the tracking error $\epsilon = ||Z - Z_0||$, representing the distance of the complex gain of the response from perfect tracking [20]. The tracking error measures the image displacement that the eyes see taking account of the head's movement, normalized by the displacement that they would see with the head fixed (Fig. 5a). Hence, whereas $\epsilon = 0$ corresponds to perfect tracking, holding the head fixed gives $\epsilon = 1$; likewise, whereas $\epsilon < 1$ corresponds to partial gaze stabilization, $\epsilon > 1$ means that the head's motion worsens gaze stability. The moths' head movements resulted in a tracking error $0.3 < \epsilon < 0.5$ at mean contrast frequencies $c \leq 3$Hz (Fig. 5b), meaning that the eyes experienced a moderate degree of apparent image displacement in each case. At higher contrast frequencies, the tracking error showed considerable and worsening variation (Fig. 5b), which reflects the large phase shift that occurred in response to high oscillation frequencies and high spatial frequencies (Fig. 3e,h). In the worst case, at frequencies $f \geq 8$Hz, the phase shift was such that the image displacement was worse than it would have been had the head made no attempt to stabilize gaze at all ($\epsilon > 1$). Overall, the angular position of the stimulus was not particularly well stabilized under any of the test conditions, because when the gain was close to one, the phase was not close to zero, and *vice versa*.

3.3 Head movements extend motion vision to higher speeds

We next asked what effect the measured head motions would have had on the performance of the motion vision system. To answer this, we simulated the response of the model Reichardt array (Fig. 2) to each test stimulus, assuming that the head was either (i) held fixed, or (ii) moving as measured. In the head-fixed case, the array output increased with the mean contrast frequency of the stimulus, until reaching a peak then declining (Fig. 6a,d,f). This was true regardless of whether we varied the oscillation frequency, oscillation amplitude, or spatial frequency of the stimulus. The highest output amplitude was achieved for oscillating stimuli with a mean contrast frequency $c \approx 2$Hz, coinciding with the array's peak steady-state response to a steadily rotating stimulus (Fig. 2d). At higher mean contrast frequencies, the phase of the response changed rapidly, ultimately becoming unstable in the amplitude and spatial frequency tests when multiple grating wavelengths were passing each ommatidium in a single oscillation cycle (Fig. 6e,h). This phase shift was associated with distortion of the array output (Fig. S1 in electronic supplementary material); see also [16]), manifested in the diminished R^2 of the sinusoid fitted to the time-varying output of the array (Fig. 6f,i). The phase of the response did not become unstable in the oscillation frequency

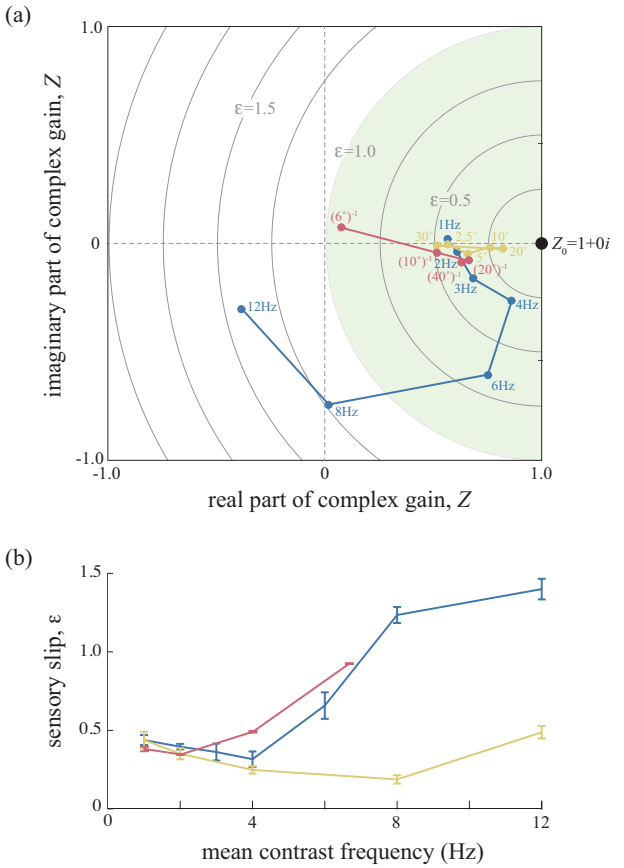

Figure 5. Mean tracking error (ϵ) of head in tests varying the frequency (blue), amplitude (golden), and spatial frequency (red) of the stimulus. (a) Plot of complex gain (Z); coloured lines interpolate adjacent test conditions. Perfect tracking with $\epsilon = 0$ corresponds uniquely to a complex gain $Z_0 = 1 + 0i$; grey isolines show the complex gains giving other values of ϵ; green shading indicates responses that assist in stabilizing gaze with $\epsilon < 1$. (b) Tracking error against mean contrast frequency, with error bars showing the mean responses $\pm$ one standard error, connected by straight line segments to aid visualisation.

tests, in which there was no significant distortion of the array output (Fig. 6c)—presumably because of the comparatively small amplitude of the oscillation relative to the wavelength of the grating; for higher amplitude to wavelength ratios, the response would be expected to become distorted at the higher oscillation frequencies [16].

The results of our simulations indicate that most of the test stimuli fell outside the range over which the open-loop output of the Reichardt array would have increased monotonically with contrast frequency, and would therefore be expected to produce distorted responses with the head held fixed (Fig. S1). Hence, the fact that the visually-modulated head motions remained consistent and coherent in response to stimulus contrast frequencies as high as $c = 12$Hz (Fig. 3) already suggests that the bandwidth of the motion vision system was extended considerably by the reduction in the apparent contrast frequency of the stimulus resulting from those same compensatory head movements. We tested this directly by simulating the effects of moving the head with the same gain and phase as we had measured experimentally under each test condition. Doing so substantially altered the output of the Reichardt array, extending its response so that the output amplitude now peaked at a mean contrast frequency some two to four times higher than with

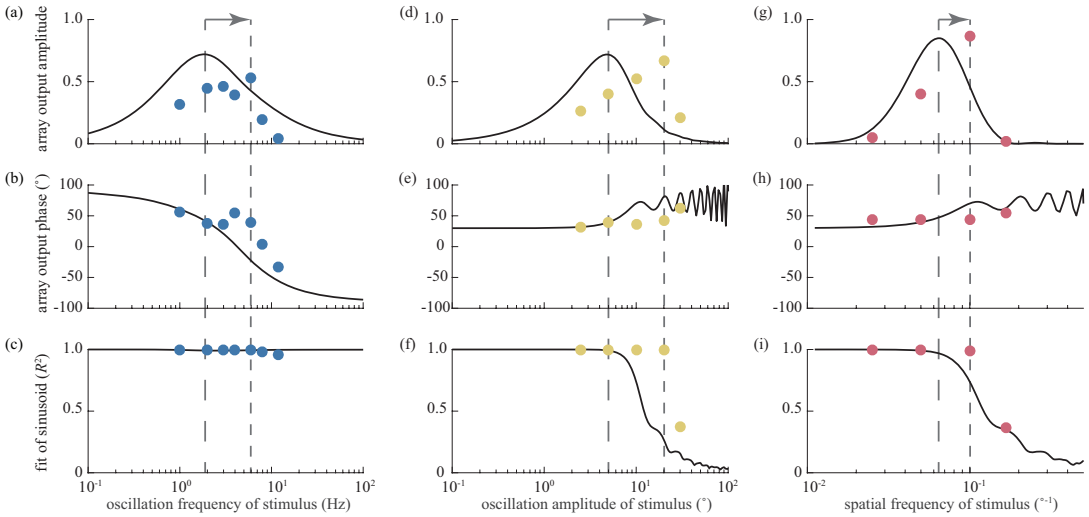

Figure 6. Response of model Reichardt array (arbitrary units) to stimuli presented in tests varying the frequency (a-c), amplitude (d-f), or spatial frequency (g-i) of the visual stimulus. Solid lines show the response with the head fixed; filled circles show the response assuming the same gain and phase of head motion as measured experimentally under each test condition. Coarse dashed lines show the peak in the head-fixed response; fine dashed lines show the peak in the response with head motion included; arrows show the resulting shift in the peak response. The amplitude, phase, and R^2 were determined by fitting a sinusoid at the stimulus frequency to the output of the array.

the head fixed, with the location of the peak depending upon whether the frequency, amplitude, or spatial frequency of the stimulus was varied (Fig. 6a,d,g). This stretching of the response curve also had the effect of pushing the onset of any substantial phase shift to higher mean contrast frequencies (Fig. 6b,e,h), and of extending the range of stimulus contrast frequencies over which a sinusoidal input still elicited a sinusoidal output (Fig. 6f,i). The picture is clearest in the tests varying the amplitude of the stimulus, which avoid the confounding effects of phase delay and spatial resolution that are inherent to the temporal and spatial frequency tests. In these tests, the moths' compensatory head movements quadrupled the effective working range of their motion vision system (Fig. 6d), with the extended response curve peaking at a mean contrast frequency $c \geq 8$Hz, compared to $c \approx 2$Hz in the head fixed case, coinciding with the onset of the breakdown in gaze stabilization (Fig. 5b).

Although it is difficult to separate cause from effect in a closed-loop system, this result makes good sense, because if compensatory head movements are driven by the output of the motion vision system, then their gain would be expected to decrease sharply at mean contrast frequencies beyond the peak in the extended response curve. This should cause a very rapid breakdown in gaze stabilization, because as the gain of the compensatory head movements becomes smaller, the reduction in the apparent contrast frequency of the stimulus becomes less pronounced. This will tend to push the motion vision system even farther beyond the peak in its response curve, leading to an even greater reduction in the gain of the compensatory head movements. The picture is more complicated for the temporal and spatial frequency tests, in which the earlier onset of the breakdown in gaze stabilization (Fig. 5b) seems to be associated with the limits imposed by phase delays and spatial resolution. In particular, although the gain of the head motions increased with the oscillation frequency of the stimulus up to a mean contrast frequency of $c = 6$Hz, the accompanying phase delay (Fig. 3b) was already sufficient to have caused a substantial impairment in gaze stabilization (Fig. 5b). The effects of phase shift also explain the irregularity of the

modified response curve in the simulations corresponding to the oscillation frequency tests (Fig. 6a), although the details are quite involved (Fig. S2 in electronic supplementary material).

4 Discussion

Although it is not necessarily surprising that compensatory head movements can extend the effective dynamic range of motion vision by attenuating the retinal slip speed of the image [4,3], the consequences of this have been almost completely ignored [22]. Here we explore these consequences, and their wider implications for the ecology of motion vision.

4.1 The motion vision system as an adaptive sensor for flight control

Our knowledge of the neurophysiology of insect motion vision derives mainly from electrophysiological preparations in which the head is fixed to permit recording from the optic lobes. This is a potentially significant limitation from the perspective of visual ecology, because the open-loop properties of the EMDs will be modified substantially when the motion vision system operates in closed-loop, with the head free to move under visual feedback. The modified response curves that we have synthesised in Fig. 6 address this by incorporating the effect of the insect's compensatory head movements in a computational model of the insect's motion vision system. In principle, these modified response curves describe the summed EMD output that we could expect to measure (were it practical to do so) in an electrophysiological preparation of a tethered insect whose head was free to move in response to a sinusoidally oscillating visual stimulus. This brings us an important step closer to characterising the output of the motion vision system under behaviourally relevant conditions than do existing electrophysiological preparations in which the head is fixed. Indeed, since rotating the visual environment with respect to the insect's body is optically equivalent to rotating the insect's body with respect to the visual environment, these modified response curves characterise precisely how the summed EMD output is expected to look in response to involuntary sinusoidal perturbations of the body in free-flight.

Such motions are important biologically because of the inherent instability of insect flight, which in hawkmoths involves certain divergent roll motions that are stabilised by visual feedback [23]. These flight stabilization responses will obviously attenuate the angular velocity of the body, but to the extent that they are driven by the motion vision system, they will only be initiated once the insect has begun to experience appreciable retinal slip. Given how much faster the head can respond relative to the body, it is reasonable to assume that this retinal slip will already have driven—and hence been modified by—the insect's compensatory head movements. Our simulations show that the visually-driven head movements observed in tethered hawkmoths attenuate the retinal slip speed enough to allow the EMDs to respond reliably to stimuli associated with self-motions four times faster than expected from their open-loop response properties alone. In *H. lineata*, this means that the EMDs should be able to encode oscillatory stimuli with mean angular rates of at least $160^\circ\ s^{-1}$ in closed-loop, compared to just $40^\circ\ s^{-1}$ in open-loop (Fig. 7a). The complete motion vision system therefore operates as an adaptive sensor, in the sense that EMD output is fed back to drive head movements which in turn serve to keep the EMDs operating within their useful working range.

This mechanism is quite general, because *any* compensatory head movement that reduces the retinal slip will serve to shift the peak output of the EMD array to higher contrast frequencies. This will increase the output of the EMDs at higher angular speeds, and decrease it at lower angular speeds, as illustrated in Fig. 7a for the case of changing stimulus oscillation amplitude. Notwithstanding the generality of this mechanism, the details of its tuning are of interest too: if the compensatory head movements used the same high gain at all speeds, then this would shift the response curve far to the right, allowing sensing of stimuli at high angular speeds, but reducing EMD output at low angular speeds for which the signal to noise ratio is already low (Fig. 7a). This reasoning suggests a clear functional explanation for the detailed

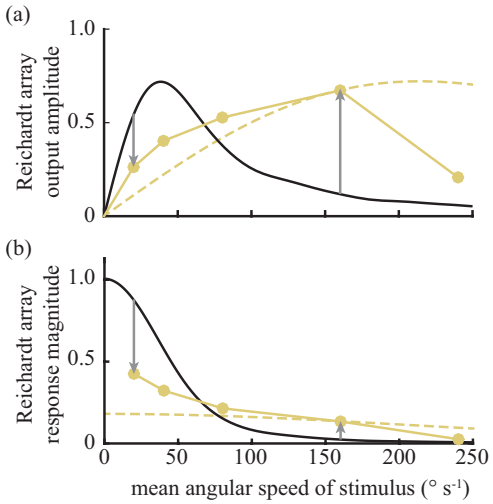

Figure 7. Response of model Reichardt array as a function of angular speed under open-loop (black lines) and closed-loop (golden lines) conditions, for the stimuli presented in the oscillation amplitude tests. Black lines show the response with the head held fixed; filled circles connected by straight line segments (golden) show the response with the head moving at the gain and phase measured experimentally for each corresponding stimulus in the oscillation amplitude tests; dashed lines (golden) show the response expected if the head were always to move at the same gain and phase as measured for the 20° amplitude stimulus. (a) Output amplitude (arbitrary units) against mean angular speed of stimulus. (b) Response magnitude (arbitrary units) against mean angular speed of stimulus, where response magnitude is defined as output amplitude normalized by stimulus speed. Compensatory head movements always reduce the retinal slip speed, increasing the output amplitude and response magnitude for fast stimuli (upward arrows), but diminishing the output amplitude and response magnitude for slow stimuli (downward arrows). Note that the output would be diminished to a far greater extent at low stimulus speeds were it not for the modulation of the gain and phase of the observed compensatory head movements (compare dashed and solid golden lines).

form of the head's magnitude response curves (Fig. 3a,d,g), which show reduced gain at low contrast frequencies—just as expected if the head's response were tuned to minimise the diminution of the EMDs' response at low stimulus speeds. In fact, the EMDs' nonlinear response properties provide a further form of automatic gain control [16,11], wherein the magnitude of their response relative to the speed of the stimulus is higher at lower stimulus speeds (Fig. 7b). When taken in combination with the effect of the compensatory head movements, the net effect of this adaptive sensing arrangement is to extend the upper limits to the performance of the moth's motion vision system (Fig. 7a) whilst maintaining sensitivity at its lower limits (Fig. 7b). This feedback mechanism is distinct from the feedforward control of head movements during voluntary manoeuvres [6,3], which may also help keep the retinal slip speed within the working range of the motion vision pathway.

Extending the performance of the motion vision system in this way has important consequences for flight control. Our earlier work [23] showed that the natural flight dynamics of hovering *H. lineata* are inherently unstable, with small roll perturbations growing exponentially with a doubling time of 0.1 s. Given that these unstable motions are stabilized by roll moments driven by feedback from the visual system, the open-loop response properties of the EMDs seem rather slow to deal with these roll instabilities, which are expected to produce 100° s^{-1} of angular velocity for every 6° of angular displacement [23]. In contrast, the closed-loop response properties of the EMDs look entirely appropriate

to provide the feedback needed for flight stabilization when the head is free to move (Fig. 7a). A similar adaptive sensing arrangement might therefore find use in small autonomous air vehicles using visual feedback for flight control, although the details of the implementation will depend upon the EMD scheme used to compute local image motion.

4.2 Implications for the ecology of motion vision

Our model of the motion vision system was tuned to electrophysiological data from *M. sexta* rather than *H. lineata*, but the underlying mechanism of gain control (Fig. 7a) is so general that we could hardly have reached any qualitatively different conclusion as a result. Nevertheless, the adaptive significance of this mechanism may be expected to vary strongly with visual ecology. The motion-sensitive interneurons of hawkmoths are tuned to respond to visual stimuli an order of magnitude slower than those of Diptera, Hymenoptera, and other Lepidoptera [17,18]. This is usually attributed to selection for an ability to stabilize slow drift when hovering at flowers [17,18], and to the constraints upon spatiotemporal acuity that are inherent to nocturnal and crepuscular vision [19–21]. Nevertheless, this slowness would be severely limiting in relation to flight control at higher image speeds were it not for the gain control mechanism that we have described. Compensatory head movements may therefore be especially significant in extending the dynamic range of the motion vision system in nocturnal and crepuscular species (see sensitivity analysis in electronic supplementary material), in which the photoreceptors are expected to be characteristically slow [27].

Looking more broadly, visually-guided eye movements form an integral part of the motion vision systems of most animals. Both the full-field tracking associated with optokinetic responses and the small-field tracking associated with smooth pursuit responses reduce the variance of the image velocity over the entire visual field [28], so it is inevitable that the open-loop response properties of the motion-sensitive neurons that drive these responses will be modified when they are operating in closed-loop. For instance, a large part of the response variability in recordings from single motion-sensitive neurons in the primary visual cortex (V1) of monkeys is attributable to fixational eye movements [29], and it has recently been suggested that the very different spatiotemporal tuning of the V1 neurons of mice may be related to their much more limited eye movements [30]. This being so, future studies of how motion-sensitive interneurons are matched to visual ecology across a broad range of organisms will need to consider their tuning in the context of the closed-loop systems of which they are a part.

Data, code and materials. Data and code available from the Dryad Digital Repository: http://dx.doi.org/10.5061/dryad.05sg7 [31].
Competing interests. We have no competing interests.
Authors' contributions. GT conceived the study. SW designed and conducted experiments. SW and GT analysed data, prepared figures, and wrote the paper.
Funding. The research leading to these results has received funding from the European Research Council under the European Community's Seventh Framework Programme (FP7/2007-2013)/ERC grant agreement no. 204513. The virtual reality flight simulator was built under BBSRC Research Grant BB/C518573/1. This material is based on research sponsored by the Air Force Research Laboratory, under agreement number FA-9550-14-1-0068 subaward number 8617-Z8145001.
Acknowledgments We thank Richard Bomphrey, Tony Price, and John Hogg for their help in designing and constructing the flight simulator.

References

1. Land MF & Nilsson DE. 2012 *Animal Eyes*. Oxford University Press.
2. Cronin TW, Johnsen S, Marshall NJ & Warrant EJ. 2014 *Visual Ecology*. Princeton University Press.
3. Hardcastle BJ & Krapp HG. 2016 Evolution of biological image stabilization. *Curr. Biol.* **26**, R1010–R1021.
4. Hengstenberg R, Sandeman D & Hengstenberg B. 1986 Compensatory head roll in the blowfly *Calliphora* during flight. *Proc. R. Soc. B* **227**, 455–482.
5. Boeddeker N & Hemmi JM. 2010 Visual gaze control during peering flight manoeuvres in honeybees. *Proc. R. Soc. B* **277**, 1209–1217.
6. Viollet S & Zeil J. 2013 Feed-forward and visual feedback control of head roll orientation in wasps (*Polistes humilis*, Vespidae, Hymenoptera). *J. Exp. Biol.* **216**, 1280–1291.
7. Taylor GK & Krapp HG. 2007 Sensory systems and flight stability: what do insects measure and why? *Adv. in Insect Physiol.* **34**, 231–316.
8. Maisakms, Haag J, Ammer G, Serbe E, Meier M, Leonhardt A, Schilling T, Bahl A, Rubin GM, Nern, A. *et al.* 2013 A directional tuning map of *Drosophila* elementary motion detectors. *Nature* **500**, 212–216.
9. Takemura S-Y, Bharioke A, Lu Z, Nern A, Vitaladevuni S, Rivlin PK, Katz WT, Olbris DJ, Plaza SM, Winston P. *et al.* 2013 A visual motion detection circuit suggested by *Drosophila* connectomics. *Nature* **500**, 175–181.
10. Egelhaaf M & Borst A. 1989 Transient and steady-state response properties of movement detectors. *J. Opt. Soc. Am. A* **6**, 116–127.
11. Borst A, Flanagin VL & Sompolinsky H. 2005 Adaptation without parameter change: dynamic gain control in motion detection. *Proc. Natl. Acad. Sci. USA* **102**, 6172–6176.
12. Hassenstein B & Reichardt W. 1956 Systemtheoretische Analyse der Zeit-, Reihenfolgen- und Vorzeichenauswertung bei der Bewegungsperzeption des Rüsselkäfers *Chlorophanus*. *Z. Naturforschg.* **11b**, 513–524.
13. Buchner E. 1984 Behavioural analysis of spatial vision in insects. In *Photoreception and Vision in Invertebrates* (ed. MA Ali), pp561–621. New York: Plenum Press.
14. Borst A, Haag J & Reiff DF. 2010 Fly motion vision. *Annu. Rev. Neurosci.* **33**, 49–70.
15. Zanker JM, Srinivasan MV & Egelhaaf M. 1999 Speed tuning in elementary motion detectors of the correlation type. *Biol. Cybern.* **80**, 109–116.
16. Egelhaaf M & Reichardt W. 1987 Dynamic response properties of movement detectors: theoretical analysis and electrophysiological investigation in the visual system of the fly. *Biol. Cybern.* **56**, 69–87.
17. O'Carroll DC, Bidwell NJ, Laughlin SB & Warrant EJ. 1996 Insect motion detectors matched to visual ecology. *Nature* **382**, 63–66.
18. O'Carroll DC, Laughlin SB, Bidwell NJ & Harris RA. 1997 Spatio-temporal properties of motion detectors matched to low image velocities in hovering insects. *Vision Res.* **37**, 3427–3439.
19. Theobald JC, Warrant EJ & O'Carroll DC. 2010 Wide-field motion tuning in nocturnal hawkmoths. *Proc. Roy. Soc. B* **277**, 853–860.
20. Sponberg S, Dyhr JP, Hall RW & Daniel TL. 2015 Luminance-dependent visual processing enables moth flight in low light. *Science* **348**, 1245–1248.
21. Stöckl AL, OCarroll DC & Warrant EJ. 2016 Neural summation in the hawkmoth visual system extends the limits of vision in dim light. *Curr. Biol.* **26(6)**, 821–826.
22. Eckert MP & Zeil J. 2001 Towards an ecology of motion vision. In *Motion Vision—Computational, Neural, and Ecological Constraints* (eds. JM Zanker & J Zeil), pp333–369. Berlin: Springer-Verlag.

23. Windsor SP, Bomphrey RJ & Taylor GK. 2014 Vision-based flight control in the hawkmoth *Hyles lineata*. *J. R. Soc. Interface* **11**, 20130921.
24. Tischler MB & Remple RK. 2006 *Aircraft and Rotorcraft System Identification: Engineering Methods with Flight-test Examples*. Reston, VA: AIAA.
25. Land MF. 1997 Visual acuity in insects. *Annu. Rev. Entomol.* **42(1)**, 147–177.
26. O'Carroll DC & Warrant EJ. 2011 Computational models for spatiotemporal filtering strategies in insect motion vision at low light levels. In *Intelligent Sensors, Sensor Networks and Information Processing (ISSNIP), 2011 Seventh International Conference, Adelaide, SA, Australia*, 119–124. IEEE.
27. Laughlin SB & Weckström M. 1993 Fast and slow photoreceptors—a comparative study of the functional diversity of coding and conductances in the Diptera. *J. Comp. Physiol. A* **172**, 593–609.
28. Eckert MP & Buchsbaum G. 1993 Effect of tracking strategies on the velocity structure of two-dimensional image sequences. *J. Opt. Soc. Am. A* **10**, 1582–1585.
29. Gur M, Beylim A & Snodderly DM. 1997 Response variability of neurons in primary visual cortex (V1) of alert monkeys. *J. Neurosci.* **17**, 2914–2920.
30. LeDue EE, Zou MY & Crowder NA. 2012 Spatiotemporal tuning in mouse primary visual cortex. *Neurosci. Lett.* **528**, 165–169.
31. Windsor SP & Taylor GK. 2017. Data from: Head movements quadruple the range of speeds encoded by the insect motion vision system in hawkmoths. Dryad Digital Repository. doi:10.5061/dryad.05sg7